Available online at www.sciencedirect.com
SCIENCE DIRECT®
Theoretical and Applied Fracture Mechanics 39 (2003) 169–180
theoretical and applied fracture mechanics
www.elsevier.com/locate/tafmec

Crack bifurcation predicted for dynamic anti-plane collinear cracks in piezoelectric materials using a non-local theory

Z.G. Zhou *, Y.G. Sun, B. Wang

Center for Composite Materials and Electro-Optics, Technology Center, Harbin Institute of Technology, P.O. Box 2147, Harbin 150001, PR China

Abstract

A non-local theory of elasticity is applied to obtain the dynamic interaction between two collinear cracks in the piezoelectric materials plane under anti-plane shear waves for the permeable crack surface boundary conditions. Unlike the classical elasticity solution, a lattice parameter enters into the problem that make the stresses and the electric displacements finite at the crack tip. A one-dimensional non-local kernel is used instead of a two-dimensional one for the anti-plane dynamic problem to obtain the stress and electric displacement near the crack tips. By means of the Fourier transform, the problem can be solved with the help of two pairs of triple integral equations in which the unknown variable is the jump of the displacement across the crack surface. The solutions are obtained by means of the Schmidt method. Crack bifurcation is predicted using the strain energy density criterion. Minimum values of the strain energy density functions are assumed to coincide with the possible locations of fracture initiation. Bifurcation angles of $\pm 5°$ and $\pm 175°$ are found. The result of possible crack bifurcation was not expected before hand.

Keywords: Crack; Elastic waves; Non-local theory; Piezoelectric materials; Fourier integral transform; Schmidt method

1. Introduction

It is well known that the piezoelectric materials produce an electric field when deformed, and undergo deformation when subjected to an electric field. The coupling nature of piezoelectric materials has attracted wide applications in electric-mechanical and electric devices, such as electric-mechanical actuators, sensors and structures. When subjected to mechanical and electrical loads in service, these piezoelectric materials can fail prematurely due to their brittleness and by the presence of defects or flaws produced during their manufacturing process. Therefore, it is important to study the electro-elastic interaction and fracture behavior of piezoelectric materials, especially when multiple cracks are involved.

In theoretical studies of crack problems, several different electric boundary conditions at the crack surfaces have been proposed by numerous researchers [1–7]. The crack surfaces being

* Corresponding author. Tel.: +86-451-641-4145; fax: +86-451-623-8476.
E-mail address: zhouzhg@hope.hit.edu.cn (Z.G. Zhou).

0167-8442/03/$ - see front matter © 2002 Elsevier Science Ltd. All rights reserved.
doi:10.1016/S0167-8442(02)00157-X

impermeable to electric fields were adopted in [1,2,4,5]. The impermeable crack assumption refers to crack surfaces that are free of surface charge and thus the electric displacement vanishes insides the crack. Cracks in the piezoelectric materials may consist of vacuum, air or some other gas. Electric fields can thus propagate through the crack such that the electric displacement component perpendicular to the crack surfaces could be continuous across the crack surfaces as in [3,6,7] where electric boundary conditions at the crack surfaces were considered. It is interesting to note that very different results were obtained by changing the boundary conditions. However, these solutions contain stress and electric displacement singularity. The state of stress near the tip of a sharp line crack in an elastic plane for non-local theories using a uniform tension, shear and anti-plane shear were discussed in [8–10]. These solutions gave finite stresses at the crack tip. The solutions in [8–10], however, were not exact and were reexamined in [11–13] using a different approach. Recently [14,15], the state of the dynamic stress near the tip of a line crack or two line cracks in an elastic plane were investigated by use of non-local theory. These solutions did not contain any stress singularity.

In the present paper, the scattering of harmonic elastic anti-plane shear waves by two collinear symmetrical permeable cracks in the piezoelectric materials is investigated by use of non-local theory. The traditional concept of linear elastic fracture mechanics and the non-local theory are extended to include the piezoelectric effects. To overcome the mathematics difficulties, some assumptions as in [16,17] were invoked. A one-dimensional non-local kernel function is used instead of a two-dimensional kernel function for the anti-plane dynamic problem to obtain the stress and electric displacement occur at the crack tips. Fourier transform technology is applied and a mixed boundary value problem is reduced to two pairs of triple integral equations. In solving the triple integral equations, the jump of the displacement across the crack surface is expanded in a series of Jacobi polynomials. This process is quite different from those adopted in the previous works as mentioned above [1–4,6–10]. As expected, the solution in this paper does not contain the stress and electric displacement singularity at the crack tip. The stress field and the electric field for the non-local theory are similar to that of the classical elasticity solution away from the crack tips. Near the crack tip, a lattice parameter tends to control the amplitude of the stress, the electric displacement and the energy density. The energy density results are used to examine the crack initiation characteristics.

2. Non-local piezoelectric materials

For the anti-plane shear problem, the basic equations of linear, homogeneous, isotropic, non-local piezoelectric materials, with vanishing body force are [6,8–10]

$$\frac{\partial \tau_{xz}}{\partial x}+\frac{\partial \tau_{yz}}{\partial y}=\rho\frac{\partial^2 w}{\partial t^2} \tag{1}$$

$$\frac{\partial D_x}{\partial x}+\frac{\partial D_y}{\partial y}=0 \tag{2}$$

$$\tau_{kz}(X,t)=\int_V [c'_{44}(|X'-X|)w_{,k}(X',t) + e'_{15}(|X'-X|)\phi_{,k}(X',t)]\,\mathrm{d}V(X') \quad (k=x,y) \tag{3}$$

$$D_k(X,t)=\int_V [e'_{15}(|X'-X|)w_{,k}(X',t) - \varepsilon'_{11}(|X'-X|)\phi_{,k}(X',t)]\,\mathrm{d}V(X') \quad (k=x,y) \tag{4}$$

where the only difference from the classical electroelastic theory is that the stress $\tau_{zk}(X,t)$ and the electric displacement $D_k(X,t)$ at a point X depends on $w_{,k}(X,t)$ and $\phi_{,k}(X,t)$, at all points of the body. w and ϕ are the mechanical displacement and electric potential. For homogeneous and isotropic piezoelectric materials there exist only three material parameters, $c'_{44}(|X'-X|)$, $e'_{15}(|X'-X|)$ and $\varepsilon'_{11}(|X'-X|)$ which are functions of the distance $|X'-X|$. ρ is the density of the piezoelectric materials. The integrals in (3) and (4) are over the volume V of the body enclosed within a surface ∂V.

As discussed in the papers [18,19], the form of $c'_{44}(|X'-X|)$, $e'_{15}(|X'-X|)$ and $\varepsilon'_{11}(|X'-X|)$ can be expressed

$$(c'_{44}, e'_{15}, \varepsilon'_{11}) = (c_{44}, e_{15}, \varepsilon_{11})\alpha(|X'-X|) \tag{5}$$

where $\alpha(|X'-X|)$ is known as the influence function and is a function of the distance $|X'-X|$, c_{44}, e_{15} and ε_{11} are the shear modulus, piezoelectric coefficient and dielectric parameter, respectively.

Substitution of Eq. (5) into Eqs. (3) and (4) yields

$$\tau_{kz}(X,t) = \int_V \alpha(|X'-X|)\sigma_{kz}(X',t)\,\mathrm{d}V(X') \quad (k=x,y) \tag{6}$$

$$D_k(X,t) = \int_V \alpha(|X'-X|)D^c_k(X',t)\,\mathrm{d}V(X') \quad (k=x,y) \tag{7}$$

where

$$\sigma_{kz} = c_{44}w_{,k} + e_{15}\phi_{,k} \tag{8}$$

$$D^c_k = e_{15}w_{,k} - \varepsilon_{11}\phi_{,k} \tag{9}$$

The expressions (8) and (9) are the classical constitutive equations.

3. The crack model

It is assumed that there are two collinear symmetric cracks of length $1-b$ along the x-axis in the piezoelectric materials plate as shown in Fig. 1. $2b$ is the distance between the two cracks. In this paper, the harmonic anti-plane shear wave is vertically incident. Let ω be the circular frequency of the incident wave. $-\tau_0$ is a magnitude of the incident wave. In what follows, the time dependence of all field quantities assumed to be of the form $\mathrm{e}^{-\mathrm{i}\omega t}$ will be suppressed but understood. It is further supposed that the two surfaces of the crack do not come in contact during vibrations. The solution of two collinear symmetric cracks of arbitrary finite length can easily be obtained by a simple change in the numerical values of the present problem. The piezoelectric boundary-value problem for anti-plane shear is considerably simplified if the out-of-plane displacement and the in-plane electric fields were only considered. Since no opening displacement exists for the present anti-plane problem, the crack surfaces can be assumed to be in perfect contact. Accordingly, permeable condition will be enforced in the present study, i.e., both the electric potential and the normal electric displacement are assumed to be continuous across the crack surfaces. So the boundary conditions of the present problem are

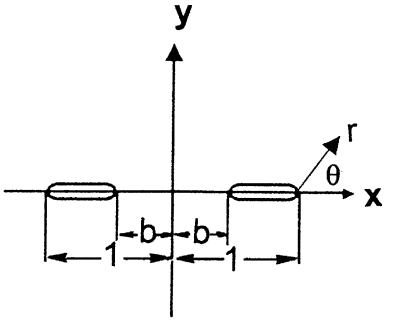

Fig. 1. Cracks in the piezoelectric materials.

$$\tau^{(1)}_{yz}(x,0^+,t) = \tau^{(2)}_{yz}(x,0^-,t) = -\tau_0, \quad b \leqslant |x| \leqslant 1 \tag{10}$$

$$\begin{aligned} &D^{(1)}_y(x,0^+,t) = D^{(2)}_y(x,0^-,t),\\ &\phi^{(1)}(x,0^+,t) = \phi^{(2)}(x,0^-,t), \quad |x| \leqslant \infty \end{aligned} \tag{11}$$

$$\begin{aligned} &w^{(1)}(x,0^+,t) = w^{(2)}(x,0^-,t) = 0,\\ &\quad 0 < |x| < b, \quad 1 < |x| \end{aligned} \tag{12}$$

$$\begin{aligned} &w^{(k)}(x,y,t) = \phi^{(k)}(x,y,t) = 0,\\ &\quad \text{for } (x^2+y^2)^{1/2} \to \infty \quad (k=1,2) \end{aligned} \tag{13}$$

Note that all quantities with superscript k ($k=1$, 2) refer to the upper half-plane and lower half-plane. Substituting Eqs. (6) and (7) into Eqs. (1) and (2), respectively, using Green–Gauss theorem, it can be obtained [10]

$$\begin{aligned} &\int_V \int \alpha(|x'-x|,|y'-y|)[c_{44}\nabla^2 w(x',y',t)\\ &\quad + e_{15}\nabla^2\phi(x',y',t)]\,\mathrm{d}x'\,\mathrm{d}y' - \left(\int_{-1}^{-b} + \int_b^1\right)\\ &\quad \times \alpha(|x'-x|,0)\big[\sigma_{yz}(x',0,t)\big]\,\mathrm{d}x' = \rho\frac{\partial^2 w}{\partial t^2} \end{aligned} \tag{14}$$

$$\int_V \int \alpha(|x'-x|,|y'-y|)[e_{15}\nabla^2 w(x',y',t) - \varepsilon_{11}\nabla^2\phi(x',y',t)]\,\mathrm{d}x'\,\mathrm{d}y' - \left(\int_{-1}^{-b} + \int_b^1\right) \times \alpha(|x'-x|,0)\llbracket D_y^c(x',0,t)\rrbracket\,\mathrm{d}x' = 0 \tag{15}$$

where the boldface bracket indicates a jump at the crack line, i.e.

$$\llbracket \sigma_{yz}(x',0,t)\rrbracket = \sigma_{yz}(x',0^+,t) - \sigma_{yz}(x',0^-,t)$$

$\nabla^2 = \partial^2/\partial x^2 + \partial^2/\partial y^2$ is the two dimensional Laplace operator. Under the applied anti-plane shear load on the unopened surfaces of the crack, the displacement field and the electric potential possess the following symmetry regulations

$$\begin{aligned} w(x,-y,t) &= -w(x,y,t),\\ \phi(x,-y,t) &= -\phi(x,y,t) \end{aligned} \tag{16}$$

Using Eq. (16), it can be found that

$$\llbracket \sigma_{yz}(x,0,t)\rrbracket = 0 \tag{17}$$

$$\llbracket D_y^c(x,0,t)\rrbracket = 0 \tag{18}$$

Hence the line integrals in (14) and (15) vanish. By taking the Fourier transform of (14) and (15) with respect to x', it can be shown that

$$\int_0^\infty \bar{\alpha}(|s|,|y'-y|)\left\{c_{44}\left[\frac{\mathrm{d}^2\bar{w}(s,y',t)}{\mathrm{d}y^2} - s^2\bar{w}(s,y',t)\right] + e_{15}\left[\frac{\mathrm{d}^2\bar{\phi}(s,y',t)}{\mathrm{d}y^2} - s^2\bar{\phi}(s,y',t)\right]\right\}\mathrm{d}y' = -\rho\omega^2\bar{w} \tag{19}$$

$$\int_0^\infty \bar{\alpha}(|s|,|y'-y|)\left\{e_{15}\left[\frac{\mathrm{d}^2\bar{w}(s,y',t)}{\mathrm{d}y^2} - s^2\bar{w}(s,y',t)\right] - \varepsilon_{11}\left[\frac{\mathrm{d}^2\bar{\phi}(s,y',t)}{\mathrm{d}y^2} - s^2\bar{\phi}(s,y',t)\right]\right\}\mathrm{d}y' = 0 \tag{20}$$

Here a superposed bar indicates the Fourier transform, e.g.

$$\bar{f}(s,y) = \int_0^\infty f(x,y)\exp(\mathrm{i}sx)\,\mathrm{d}x$$

What now remains is to solve the integrodifferential equations (19) and (20) for the function w and ϕ. It seems obvious that a rigorous solution of such a problem encounters serious if not unsurmountable mathematical difficulties, and one has to resort to an approximate procedure. In this given problem, according to the assumptions as in [16,17] papers, the non-local interaction in y-direction can be ignored. It can be given

$$\bar{\alpha}(|s|,|y'-y|) = \bar{\alpha}_0(s)\delta(y'-y) \tag{21}$$

From Eqs. (19) and (20), it can be shown that

$$\bar{\alpha}_0(s)\left\{c_{44}\left[\frac{\mathrm{d}^2\bar{w}(s,y,t)}{\mathrm{d}y^2} - s^2\bar{w}(s,y,t)\right] + e_{15}\left[\frac{\mathrm{d}^2\bar{\phi}(s,y,t)}{\mathrm{d}y^2} - s^2\bar{\phi}(s,y,t)\right]\right\} = -\rho\omega^2\bar{w} \tag{22}$$

$$e_{15}\left[\frac{\mathrm{d}^2\bar{w}(s,y,t)}{\mathrm{d}y^2} - s^2\bar{w}(s,y,t)\right] - \varepsilon_{11}\left[\frac{\mathrm{d}^2\bar{\phi}(s,y,t)}{\mathrm{d}y^2} - s^2\bar{\phi}(s,y,t)\right] = 0 \tag{23}$$

The general solutions of Eqs. (22) and (23) satisfying (13) are, respectively,

$$w^{(1)}(x,y,t) = \frac{2}{\pi}\int_0^\infty A_1(s)\mathrm{e}^{-\gamma y}\cos(xs)\,\mathrm{d}s, \quad y \geqslant 0 \tag{24}$$

$$\phi^{(1)}(x,y,t) - \frac{e_{15}}{\varepsilon_{11}}w^{(1)}(x,y,t) = \frac{2}{\pi}\int_0^\infty B_1(s)\mathrm{e}^{-sy}\cos(xs)\,\mathrm{d}s, \quad y \geqslant 0 \tag{25}$$

$$w^{(2)}(x,y,t) = \frac{2}{\pi}\int_0^\infty A_2(s)\mathrm{e}^{\gamma y}\cos(xs)\,\mathrm{d}s, \quad y \leqslant 0 \tag{26}$$

$$\phi^{(2)}(x,y,t) - \frac{e_{15}}{\varepsilon_{11}}w^{(2)}(x,y,t) = \frac{2}{\pi}\int_0^\infty B_2(s)\mathrm{e}^{sy}\cos(xs)\,\mathrm{d}s, \quad y \leqslant 0 \tag{27}$$

where $\gamma^2 = s^2 - \omega^2/c^2\bar{\alpha}_0(s)$, $c^2 = \mu/\rho$ and $\mu = c_{44} + e_{15}^2/\varepsilon_{11}$. $A_1(s)$, $B_1(s)$, $A_2(s)$ and $B_2(s)$ are unknown functions to be determined by the boundary conditions. For solving the problem, the jump func-

tions of the displacements and the electric potentials across the crack surfaces are defined as follows

$$f_w(x) = w^{(1)}(x,0^+,t) - w^{(2)}(x,0^-,t),$$
$$f_\phi(x) = \phi^{(1)}(x,0^+,t) - \phi^{(2)}(x,0^-,t) \tag{28}$$

Substituting (24)–(27) into (28), and applying the Fourier transform, it can be obtained

$$\bar{f}_w(s) = A_1(s) - A_2(s),$$
$$\bar{f}_\phi(s) = \frac{e_{15}}{\varepsilon_{11}}[A_1(s) - A_2(s)] + B_1(s) - B_2(s) \tag{29}$$

Substituting Eqs. (27) and (28) into Eqs. (10)–(12), it can be obtained

$$-\mu\gamma[A_1(s) + A_2(s)] - e_{15}s[B_1(s) + B_2(s)] = 0,$$
$$B_1(s) + B_2(s) = 0 \tag{30}$$

$$\frac{e_{15}}{\varepsilon_{11}}[A_1(s) - A_2(s)] + B_1(s) - B_2(s) = 0 \tag{31}$$

By solving four Eqs. (29)–(31) with four unknown functions and applying the boundary conditions (10) and (11), it can be obtained

$$\frac{1}{\pi}\int_0^\infty \bar{\alpha}_0(s)\left[\mu\gamma - \frac{e_{15}^2}{\varepsilon_{11}}s\right]\bar{f}_w(s)\cos(sx)\,\mathrm{d}s = \tau_0,$$
$$b \leqslant |x| \leqslant 1 \tag{32}$$

$$\frac{1}{\pi}\int_0^\infty \bar{f}_w(s)\cos(sx)\,\mathrm{d}s = 0, \quad 0 < |x| < b, \quad 1 < |x| \tag{33}$$

and $\bar{f}_\phi(s) = 0$, $f_\phi(x) = 0$ for all s and x. To determine the unknown function $\bar{f}_w(s)$, the triple integral equations (32) and (33) must be solved.

4. Solution of the triple integral equation

The triple integral equations (32) and (33) cannot be transformed into Fredholm integral equation of the second kind as in [9,10], because the kernel of Fredholm integral equation of the second kind in [9,10] is divergent. In [9,10], the Fredholm integral equation of the second kind can be rewritten as following

$$h(x) + \int_0^1 h(u)L(x,u)\,\mathrm{d}u = g(x)$$

where $g(x)$ is known function, $h(x)$ is unknown function.

The kernel of Fredholm integral equation of the second kind in [10] can be written as follows:

$$L(x,u) = (xu)^{1/2}\int_0^\infty tk(\varepsilon' t)J_0(xt)J_0(ut)\,\mathrm{d}t,$$
$$0 \leqslant x, \quad u \leqslant 1$$

where $J_n(x)$ is the Bessel function of order n.

$$k(\varepsilon' t) = -\Phi(\varepsilon' t), \quad \lim_{t\to\infty} k(\varepsilon' t) \neq 0 \quad \text{for } \varepsilon' = \frac{a}{2\beta l} \neq 0$$

($l$is the length of the crack).

$$J_0(x) \approx \sqrt{\frac{2}{\pi x}}\cos\left(x - \frac{1}{4}\pi\right) \quad \text{for } x \gg 0$$

The limit of $tk(\varepsilon' t)J_0(xt)J_0(ut)$ is unequal to zero for $t \to \infty$. So the kernel $L(x,u)$ in [10] is divergent. Of course, the triple integral equations (32) and (33) can be considered to be a single integral equation of the first kind with a discontinuous kernel [8]. It is well-known in the literature that integral equations of the first kind are generally ill-posed in the sense of Hadamard, e.g. small perturbations of the data can yield arbitrarily large changes in the solution. This makes the numerical solution of such equations quite difficult. In this paper, the Schmidt method [20] was used to overcome the difficulty. As discussed in [8–10], it was taken

$$\alpha_0 = \chi_0 \exp(-(\beta/a)^2(x' - x)^2), \quad \chi_0 = \beta/a\sqrt{\pi} \tag{34}$$

where β is a constant (here $\beta = e_0\sqrt{\pi}/(1-b)$, e_0 is a constant appropriate to each material). a is the lattice parameter. So it can be obtained

$$\bar{\alpha}_0(s) = \exp(-(sa)^2/(2\beta)^2) \tag{35}$$

and $\bar{\alpha}_0(s) = 1$ for the limit $a \to 0$, so that Eqs. (32) and (33) reduce to a set of triple integral equation for the same problem in the classical theory [21]. Here the Schmidt method can be used to solve the

triple integral equations (32) and (33). The gap functions of the crack surface displacement can be represented by the following series:

$$f_w(x) = w^{(1)}(x,0^+,t) - w^{(2)}(x,0^-,t) = \sum_{n=0}^{\infty} a_n P_n^{(1/2,1/2)}\left(\frac{x-\frac{1+b}{2}}{\frac{1-b}{2}}\right)\left(1-\frac{\left(x-\frac{1+b}{2}\right)^2}{\left(\frac{1-b}{2}\right)^2}\right)^{1/2} \quad \text{for } b \leqslant x \leqslant 1, \tag{36}$$

$$f_w(x) = w^{(1)}(x,0^+,t) - w^{(2)}(x,0^-,t) = 0 \quad \text{for } 0 < x < b,\ \ 1 < x, y = 0 \tag{37}$$

where a_n is unknown coefficients to be determined and $P_n^{(1/2,1/2)}(x)$ is a Jacobi polynomial [22]. The Fourier transformation of Eq. (36) is [23]

$$\bar{f}_w(s) = \sum_{n=0}^{\infty} a_n Q_n G_n(s) \frac{1}{s} J_{n+1}\left(s\frac{1-b}{2}\right) \tag{38}$$

$$Q_n = 2\sqrt{\pi}\frac{\Gamma\left(n+1+\frac{1}{2}\right)}{n!},$$

$$G_n(s) = \begin{cases} (-1)^{n/2}\cos\left(s\frac{1+b}{2}\right), & n = 0,2,4,6,\ldots \\ (-1)^{(n+1)/2}\sin\left(s\frac{1+b}{2}\right), & n = 1,3,5,7,\ldots \end{cases} \tag{39}$$

where $\Gamma(x)$ and $J_n(x)$ are the Gamma and Bessel functions. For the non-local theory problem. Substituting Eq. (38) into Eqs. (32) and (33), Eq. (33) can be automatically satisfied, and Eq. (32) are reduced to the form

$$\sum_{n=0}^{\infty} a_n Q_n \int_0^{\infty} \bar{\alpha}_0(s)[\mu\gamma/s - e_{15}^2/\varepsilon_{11}]G_n(s) \times J_{n+1}\left(s\frac{1-b}{2}\right)\cos(sx)\,\mathrm{d}s = \pi\tau_0 \tag{40}$$

For a large s, the integrands of Eq. (40) almost decreases exponentially. So the semi-infinite integral in Eq. (40) can be evaluated numerically. Eq. (40) can now be solved for the coefficients a_n by the Schmidt method [20] as shown in Appendix A.

5. Numerical calculations

From the works in [11–13,24], it can be seen that the Schmidt method is performed satisfactorily if the first 10 terms in infinite series to Eq. (40) are retained. Although the entire perturbation stress field and the perturbation electric displacement field can be determined from coefficients a_n, it is importance in fracture mechanics to determine the dynamic the stress $\tau_{yz}^{(1)}$, the electric displacement $D_y^{(1)}$ and the volume energy density function $\mathrm{d}W^{(1)}/\mathrm{d}V$ in the vicinity of the crack tips as mentioned in [25–27]. $\tau_{yz}^{(1)}$, $D_y^{(1)}$ and $\mathrm{d}W^{(1)}/\mathrm{d}V$ can be expressed, respectively, as

$$\tau_{yz}(x,0,t) = \tau_{yz}^{(1)}(x,0,t) = -\frac{1}{\pi}\sum_{n=0}^{\infty} a_n Q_n \int_0^{\infty} \bar{\alpha}_0(s)\left[\frac{\mu\gamma}{s} - e_{15}^2/\varepsilon_{11}\right] \times G_n(s) J_{n+1}\left(s\frac{1-b}{2}\right)\cos(xs)\,\mathrm{d}s \tag{41}$$

$$D_y(x,0,t) = D_y^{(1)}(x,0,t) = -\frac{e_{15}}{\pi}\sum_{n=0}^{\infty} a_n Q_n \int_0^{\infty} \bar{\alpha}_0(s) G_n(s) \times J_{n+1}\left(s\frac{1-b}{2}\right)\cos(xs)\,\mathrm{d}s \tag{42}$$

$$\frac{\mathrm{d}W(r,\theta,t)}{\mathrm{d}V} = \frac{\mathrm{d}W^{(1)}(x,y,t)}{\mathrm{d}V} = \frac{1}{2}\tau_{xz}^{(1)}\frac{\partial w^{(1)}}{\partial x} + \frac{1}{2}\tau_{yz}^{(1)}\frac{\partial w^{(1)}}{\partial y} + \frac{1}{2}D_x^{(1)}E_x^{(1)} + \frac{1}{2}D_y^{(1)}E_y^{(1)} \tag{43}$$

where $x = 1 + r\cos\theta$, $y = r\sin\theta$ for the outer crack tip, $x = b + r\cos\theta$, $y = r\sin\theta$ for the inner crack tip (r is the polar radius and θ is the polar angle as shown in Fig. 1.). $E_x^{(1)}$ and $E_y^{(1)}$ are the electric field intensity, i.e. $E_x^{(1)} = -\partial\phi^{(1)}/\partial x$, $E_y^{(1)} = -\partial\phi^{(1)}/\partial y$.

For $a = 0$ at $x = b, 1$, the classical stress and the electric displacement singularity will occur at the crack tips. However, so long as $a \neq 0$, the semi-infinite integration and the series in Eqs. (41) and (42) are convergent for any variable x. Eqs. (41) and (42) give a finite stress, a finite electric displacement all along $y = 0$, so there is no stress and the electric displacement singularity at the crack tips. At $b < x < 1$, τ_{yz}/τ_0 is very close to unity, and for $x > 1$, τ_{yz}/τ_0 and D_y/D_0 possess finite values diminishing from a finite value at $x = 1$ to zero at

$x = \infty$. Since $a/2\beta > 1/100$ represents a crack length of less than 100 atomic distances as stated in [10], and such submicroscopic sizes other serious questions arise regarding the interatomic arrangements and force laws, the solution is not pursued at such small crack sizes. The semi-infinite numerical integrals are evaluated easily by Filon's method and Simpson methods because of the rapid diminution of the integrands. In the computations, the piezoelectric material is assumed to be the commercially available piezoelectric PZT-5H. The material constants of PZT-5H are $c_{44} = 2.3(\times 10^{10}\ \mathrm{N/m^2})$, $e_{15} = 17.0\ (\mathrm{C/m^2})$ and $\varepsilon_{11} = 150.4(\times 10^{-10}\ \mathrm{C/V\,m^2})$. The solution of two collinear cracks of arbitrary length $a - b$ can easily be obtained by a simple change in the numerical values of the present paper ($a > b > 0$), i.e., it can use the results of the collinear cracks of length $1 - b/a$ in the present paper. The solution of this paper is suitable for the arbitrary length two collinear cracks.

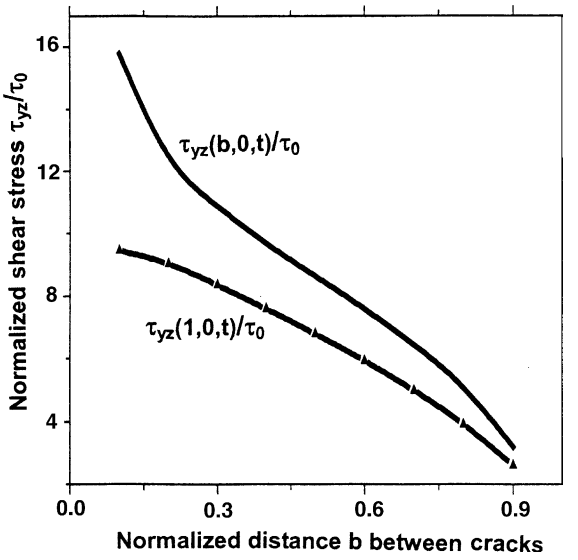

Fig. 2. The stress at the crack tip versus b for $a/2\beta = 0.001$, $\omega/c = 0.2$ (PZT-5H).

6. Discussion

The aim of the present paper was to study the application of non-local theory in fracture mechanics of the piezoelectric materials. The other aim of the present paper was to show that the Schmidt method can be used to solve this kind of the triple (dual) integral equation which the limit of the kernel does not tend to a constant. This method is more exact and more appropriate than that in [10] for the problem at hand. No stress singularity is present at the crack tip. The effects of the geometry of the interacting cracks, the frequency of the incident wave and the lattice parameter upon the dynamic stress and the electric displacement fields of the crack were examined. The volume energy density function that was proposed in [25] will be used as a fracture criterion in contrast to the Griffith's energy release rate that was found to yield unphysical results for piezoelectric materials [26,27]. The volume energy density function $\mathrm{d}W/\mathrm{d}V$ near the crack tips is thus adopted. The results of the present paper are plotted in Figs. 2–14. From the results, the following observations can be made:

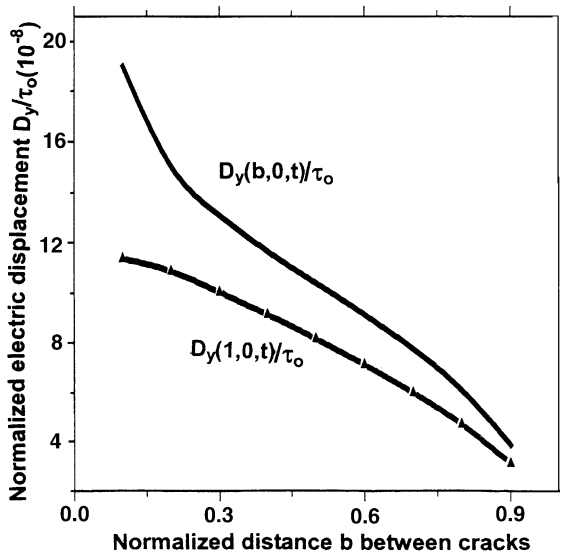

Fig. 3. The electric displacement at the crack tip versus b for $a/2\beta = 0.001$, $\omega/c = 0.2$ (PZT-5H).

(i) The maximum perturbation stress and the perturbation electric displacement do not occur at the crack tip, but slightly away from it. This phenomenon has been thoroughly substantiated in [28]. The maximum stress and the maximum

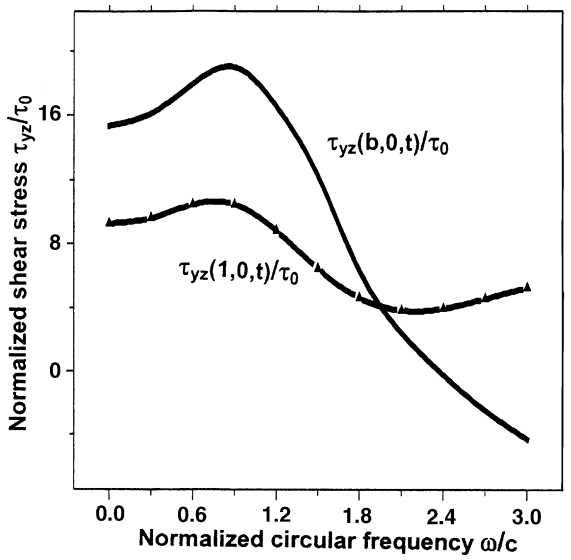

Fig. 4. The stress at the crack tip versus ω/c for $a/2\beta = 0.0001$, $b = 0.1$ (PZT-5H).

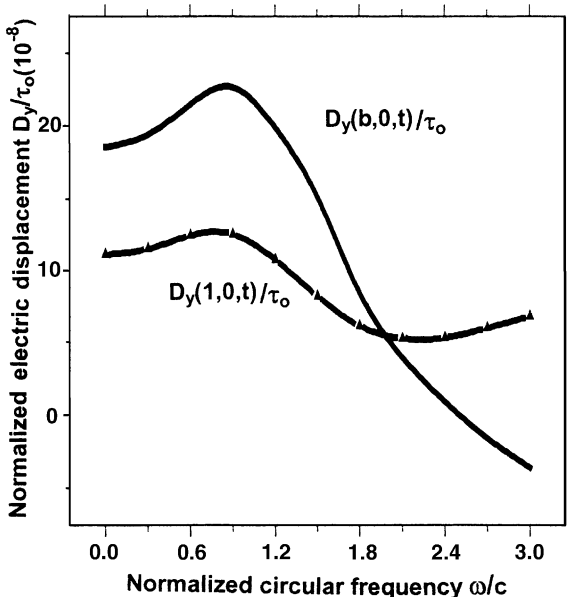

Fig. 5. The electric displacement at the crack tip versus ω/c for $b = 0.1$, $a/2\beta = 0.0001$ (PZT-5H).

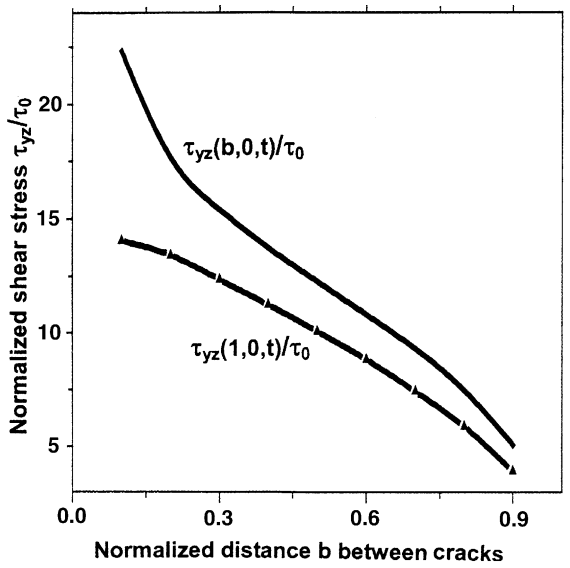

Fig. 6. The stress at the crack tip versus b for $a/2\beta = 0.0005$, $\omega/c = 0.2$ (PZT-5H).

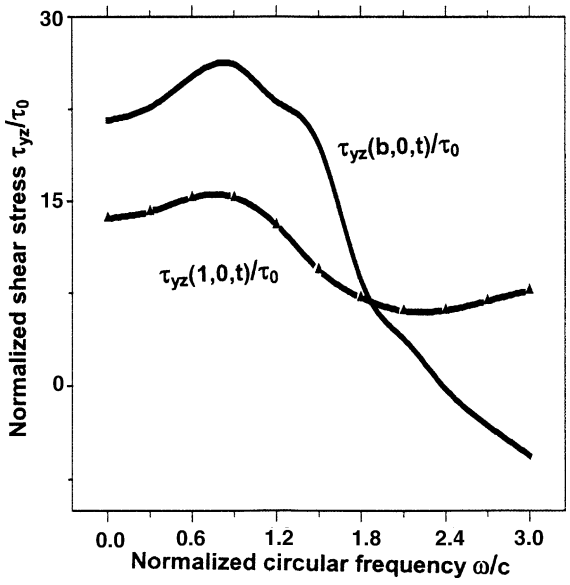

Fig. 7. The stress at the crack tip versus ω/c for $a/2\beta = 0.0005$, $b = 0.1$ (PZT-5H).

electric displacement are finite. The distance between the crack tip and the maximum stress point is very small, and it depends on the crack length and the lattice parameter. No stress and the electric displacement singularity are present at the crack tip, and also the present results converge to the classical ones when far away from the crack

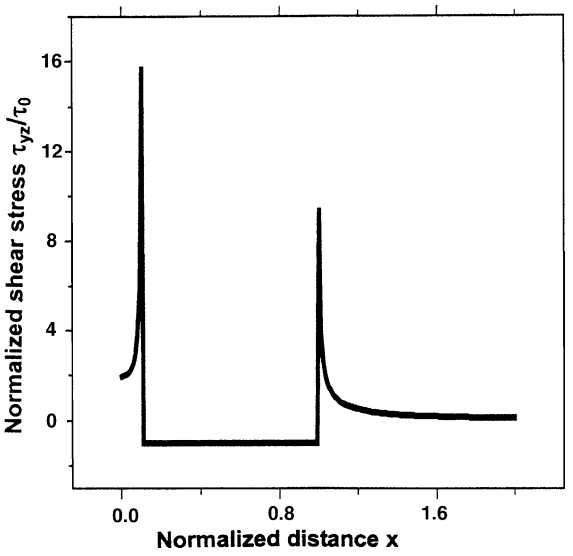

Fig. 8. The stress along the crack line versus x for $\omega/c = 0.2$, $b = 0.1$, $a/2\beta = 0.001$ (PZT-5H).

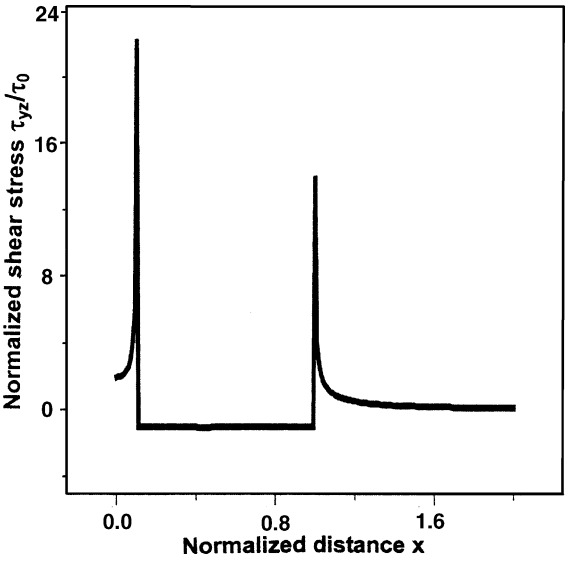

Fig. 10. The stress along the crack line versus x for $\omega/c = 0.2$, $b = 0.1$, $a/2\beta = 0.0005$ (PZT-5H).

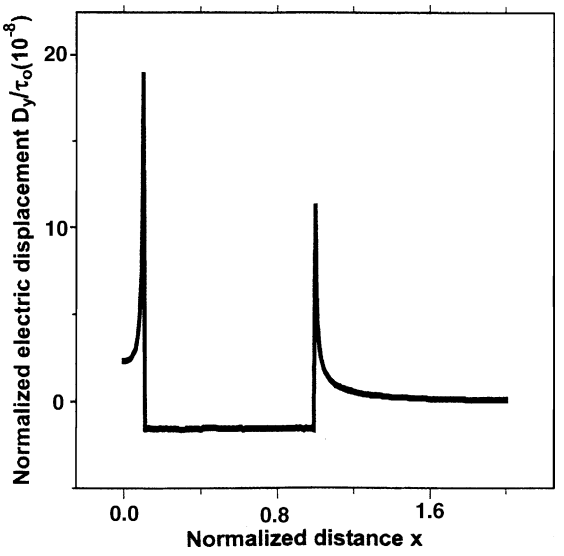

Fig. 9. The electric displacement along the crack line versus x for $\omega/c = 0.2$, $a/2\beta = 0.001$, $b = 0.1$ (PZT-5H).

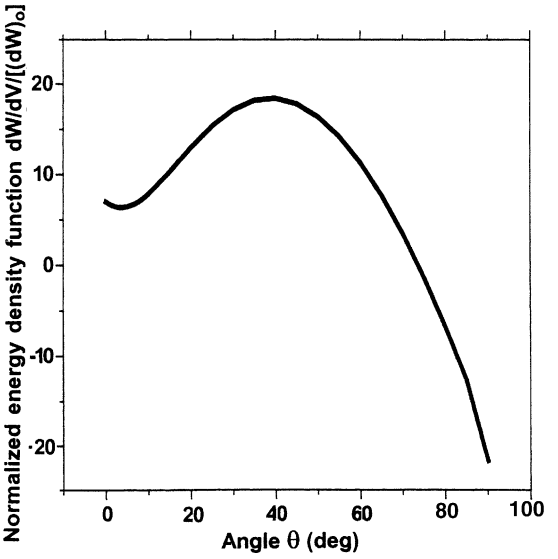

Fig. 11. Variations of dimensionless strain energy density function with polar angle for $r = 0.001$, $\omega/c = 0.3$, $a = 0.0001$, $b = 0.1$ near the outer crack tip (PZT-5H).

tip. The dynamic stress and electric displacement at the crack tip becomes infinite as the atomic distance $a \to 0$. This corresponds to the classical continuum limit of square root singularity.

(ii) The left tip's stress and the electric displacement are greater than the right tip's ones for the right crack for $\omega/c < 1.8$. Whereas, the left tip's stress and the electric displacement are smaller than the right tip's ones for the right crack for $\omega/c > 1.8$. This phenomenon should be further

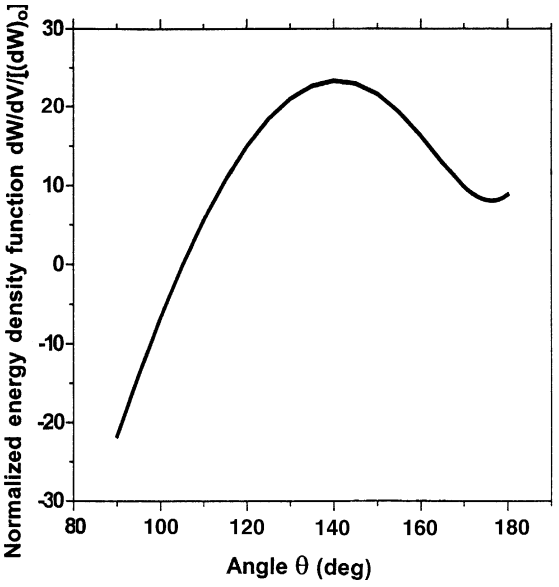

Fig. 12. Variations of dimensionless strain energy density function with polar angle for $r = 0.001$, $\omega/c = 0.3$, $a = 0.0001$, $b = 0.1$ near the inner crack tip (PZT-5H).

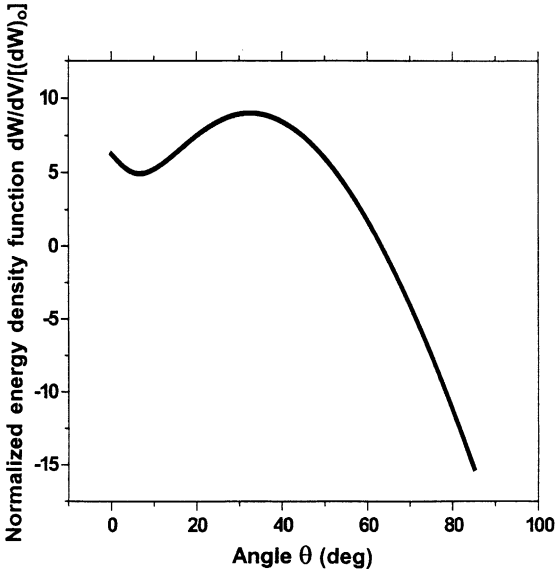

Fig. 13. Variations of dimensionless strain energy density function with polar angle for $r = 0.001$, $\omega/c = 0.3$, $a = 0.0005$, $b = 0.1$ near the outer crack tip (PZT-5H).

investigated. The stress and the electric displacement on the crack line increase with increasing of

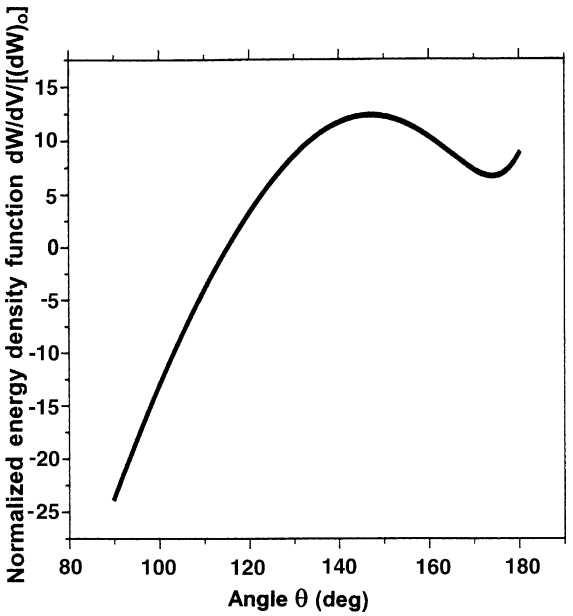

Fig. 14. Variations of dimensionless strain energy density function with polar angle for $r = 0.001$, $\omega/c = 0.3$, $a = 0.0005$, $b = 0.1$ near the inner crack tip (PZT-5H).

the length of the crack. However, the dynamic perturbation stress and the perturbation electric displacement at the crack tips tend to decrease with increasing of $a/2\beta$.

(iii) The dimensionless perturbation stress and the electric displacement depend on the length of the crack, the lattice parameter, the material parameters, the circular frequency of the incident wave and the wave velocity.

(iv) In contrast to the impermeable crack surface condition solution as shown in [29], it is found that the perturbation electric displacement field for the permeable crack surface conditions is much smaller than the results for the impermeable crack surface conditions.

(v) The dynamic perturbation stress and the electric displacement at the crack tips tend to increase with the frequency reaches a peak and then to decrease in magnitude. It can be shown that the stresses at the crack tips show a maximum value near a certain frequency. So the stress field can reach the minimum value by changing the frequency of the incident wave, the lattice parameter and the length of the crack.

(vi) For $0° < \theta < 10°$ and $170° < \theta < 180°$, the volume energy density function dW/dV near the crack tips tends to decrease with polar angle θ reaches a peak and then to increase in magnitude for the outer crack tip and the inner crack tip as shown in Figs. 11–14. The minimum value of dW/dV is found to occur at about 5° at the outer crack tip, the minimum value of dW/dV is found to occur at about 175° at the inner crack tip. Because of the symmetry, the minimum value of dW/dV will also occur at about −5° at the outer crack tip, the minimum value of dW/dV will also occur at about −175° at the inner crack tip. As discussed in [25], these can be used to predict the bifurcate direction of the crack growth under electric and mechanical combined mixed mode conditions.

(vii) For $10° < \theta < 90°$ and $90° < \theta < 170°$, the volume energy density function dW/dV near the outer crack tip and the inner crack tip tends to increase with polar angle θ reaches a peak and then to decrease in magnitude. According to the plot of the volume energy density function dW/dV versus angle θ near the crack tips, the maximum value of dW/dV is found to occur at about 35° at the outer crack tip, the maximum value of dW/dV is found to occur at about 150° at the inner crack tip.

(viii) The traditional concept of linear elastic fracture mechanics and the non-local theory can be used to solve the fracture problem in the piezoelectric materials.

Acknowledgements

The authors are grateful for financial supported by the Natural Science Foundation of Hei Long Jiang Province, the National Natural Science Foundation of China Through the Key Program (50232030), the National Natural Science Foundation of China (10172030), the Post Doctoral Science Foundation of Hei Long Jiang Province, the Multidiscipline Scientific Research Foundation of Harbin Institute of Technology (HIT.MD2001.39) and the author wishes to express his hearty thanks to Professor G. C. Sih, Lehigh University, for his invaluable suggestions.

Appendix A

For brevity, Eq. (40) can be rewritten as

$$\sum_{n=0}^{\infty} a_n E_n(x) = U(x), \quad b < x < 1 \tag{A.1}$$

where $E_n(x)$ and $U(x)$ are known functions and a_n are unknown coefficients. A set of functions $P_n(x)$ which satisfy the orthogonality condition

$$\int_b^1 P_m(x)P_n(x)\,dx = N_n\delta_{mn}, \quad N_n = \int_b^1 P_n^2(x)\,dx \tag{A.2}$$

can be constructed from the function, $E_n(x)$, such that

$$P_n(x) = \sum_{i=0}^{n} \frac{M_{in}}{M_{nn}} E_i(x) \tag{A.3}$$

where M_{ij} is the cofactor of the element d_{ij} of D_n, which is defined as

$$D_n = \begin{bmatrix} d_{00}, d_{01}, d_{02}, \ldots, d_{0n} \\ d_{10}, d_{11}, d_{12}, \ldots, d_{1n} \\ d_{20}, d_{21}, d_{22}, \ldots, d_{2n} \\ \ldots\ldots\ldots\ldots\ldots \\ \ldots\ldots\ldots\ldots\ldots \\ \ldots\ldots\ldots\ldots\ldots \\ d_{n0}, d_{n1}, d_{n2}, \ldots, d_{nn} \end{bmatrix},$$

$$d_{ij} = \int_b^1 E_i(x)E_j(x)\,dx \tag{A.4}$$

Using Eqs. (A.1)–(A.4), it can be obtained

$$a_n = \sum_{j=n}^{\infty} q_j \frac{M_{nj}}{M_{jj}} \quad \text{with } q_j = \frac{1}{N_j}\int_b^1 U(x)P_j(x)\,dx \tag{A.5}$$

References

[1] W.E.F. Deeg, The analysis of dislocation, crack and inclusion problems in piezoelectric solids, Ph.D. Thesis, Stanford University, 1980.

[2] Z. Suo, C.M. Kuo, D.M. Barnett, J.R. Willis, Fracture mechanics for piezoelectric ceramics, J. Mech. Phys. Solids. 40 (1992) 739–765.

[3] T.Y. Zhang, P. Tong, Fracture mechanics for a mode III crack in a piezoelectric material, Int. J. Solids Struct. 33 (1996) 343–359.
[4] H.A. Sosa, Y.E. Pak, Three-dimensional eigenfunction analysis of a crack in a piezoelectric ceramics, Int. J. Solids Struct. 26 (1990) 1–15.
[5] Z.G. Zhou, B. Wang, M.S. Cao, Analysis of two collinear cracks in a piezoelectric layer bonded to dissimilar half-spaces subjected to anti-plane shear, Eur. J. Mech. A/Solids 20 (2001) 213–226.
[6] A.K. Soh, D.N. Fang, K.L. Lee, Analysis of a bi-piezoelectric ceramic layer with an interfacial crack subjected to anti-plane shear and in-plane electric loading, Eur. J. Mech. A/Solid 19 (2000) 961–977.
[7] P.M. McMeeking, On mechanical stress at cracks in dielectrics with application to dielectric breakdown, J. Appl. Phys. 62 (1989) 3122–3316.
[8] A.C. Eringen, C.G. Speziale, B.S. Kim, Crack tip problem in non-local elasticity, J. Mech. Phys. Solids 25 (1977) 339–355.
[9] A.C. Eringen, Linear crack subject to shear, Int. J. Fract. 14 (1978) 367–379.
[10] A.C. Eringen, Linear crack subject to antiplane shear, Engng. Fract. Mech. 12 (1979) 211–219.
[11] Z.G. Zhou, J.C. Han, S.Y. Du, Investigation of a Griffith crack subject to anti-plane shear by using the non-local theory, Int. J. Solids Struct. 36 (1999) 3891–3901.
[12] Z.G. Zhou, S.Y. Du, J.C. Han, Non-local theory solution for in-plane shear of through crack, Theoret. Appl. Fract. Mech. 30 (1998) 185–194.
[13] Z.G. Zhou, X.W. Zhang, Y.Y. Bai, Investigation of two Griffith cracks subject to uniform tension by using the non-local theory, Int. J. Engng. Sci. 37 (1999) 1709–1722.
[14] Z.G. Zhou, B. Wang, S.Y. Du, Scattering of harmonic anti-plane shear waves by a finite crack by using the non-local theory, Int. J. Fract. 91 (1998) 13–22.
[15] Z.G. Zhou, Y.P. Shen, Investigation of the scattering of harmonic shear waves by two collinear cracks using the non-local theory, ACTA Mech. 135 (1999) 169–179.
[16] J.L. Nowinski, On non-local aspects of the propagation of love waves, Int. J. Engng. Sci. 22 (1984) 383–392.
[17] J.L. Nowinski, On non-local theory of wave propagation in elastic plates, ASME J. Appl. Mech. 51 (1984) 608–613.
[18] A.C. Eringen, Non-local elasticity and waves, in: P. Thoft-Christensen (Ed.), Continuum Mechanics Aspects of Geodynamics and Rock Fracture Mechanics, Holland, Dordrecht, 1974, pp. 81–105.
[19] A.C. Eringen, Continuum mechanics at the atomic scale, Crystal Lattice Def. 7 (1977) 109–130.
[20] P.M. Morse, H. Feshbach, in: Methods of Theoretical Physics, vol. 1, McGraw-Hill, New York, 1958.
[21] G.C. Sih, in: Mechanics of Fracture, vol. 4, Noordhoff (New Kluwer Academic), Holland, 1973.
[22] I.S. Gradshteyn, I.M. Ryzhik, Table of Integral, Series and Products, Academic Press, New York, 1980.
[23] A. Erdelyi (Ed.), Tables of Integral Transforms, vol. 1, McGraw-Hill, New York, 1954.
[24] S. Itou, Three dimensional waves propagation in a cracked elastic solid, ASME J. Appl. Mech. 45 (1978) 807–811.
[25] G.C. Sih, Mechanics of Fracture Initiation and Propagation, Kluwer Academic Publishers, Dordrecht, 1991.
[26] J.Z. Zuo, G.C. Sih, Energy density formulation and interpretation of cracking behavior for piezoelectric ceramics, Theoret. Appl. Fract. Mech. 34 (1) (2000) 17–33.
[27] G.C. Sih, J.Z. Zuo, Energy density formulation and interpretation of cracking behavior for piezoelectric ceramics, Theoret. Appl. Fract. Mech. 34 (2) (2000) 123–141.
[28] A.C. Eringen, Interaction of a dislocation with a crack, J. Appl. Phys. 54 (1983) 6811.
[29] Z.G. Zhou, S.Y. Du, B. Wang, Investigation of anti-plane shear behavior of a Griffith crack in a piezoelectric materials by using the non-local theory, Int. J. Fract. 111 (2001) 105–117.